



Uncertainty in emissions projections for climate models

M.D. Webster^{a,*}, M. Babiker^b, M. Mayer^c, J.M. Reilly^b, J. Harnisch^d, R. Hyman^b,
M.C. Sarofim^b, C. Wang^b

^aDepartment of Public Policy, University of North Carolina Chapel Hill, CB# 3435, Chapel Hill, NC 27599, USA

^bMIT Joint Program on the Science and Policy of Global Change, Massachusetts Institute of Technology, 1 Amherst St., E40-271, Cambridge, MA 02139, USA

^cAVL List GmbH, Hans List Platz 1, A-8020 GRAZ, Austria

^dECOFYS Energy & Environment, Energy Technologies Centre (ETZ), Landgrabenstrasse 100, 90459 Nuremberg, Germany

Received 3 August 2001; received in revised form 25 February 2002; accepted 25 February 2002

Abstract

Future global climate projections are subject to large uncertainties. Major sources of this uncertainty are projections of anthropogenic emissions. We evaluate the uncertainty in future anthropogenic emissions using a computable general equilibrium model of the world economy. Results are simulated through 2100 for carbon dioxide (CO₂), methane (CH₄), nitrous oxide (N₂O), hydrofluorocarbons (HFCs), perfluorocarbons (PFCs) and sulfur hexafluoride (SF₆), sulfur dioxide (SO₂), black carbon (BC) and organic carbon (OC), nitrogen oxides (NO_x), carbon monoxide (CO), ammonia (NH₃) and non-methane volatile organic compounds (NMVOCs). We construct mean and upper and lower 95% emissions scenarios (available from the authors at 1° × 1° latitude–longitude grid). Using the MIT Integrated Global System Model (IGSM), we find a temperature change range in 2100 of 0.9 to 4.0°C, compared with the Intergovernmental Panel on Climate Change emissions scenarios that result in a range of 1.3 to 3.6°C when simulated through MIT IGSM. © 2002 Elsevier Science Ltd. All rights reserved.

Keywords: Atmospheric chemistry; Monte Carlo simulation; Air pollution; Economic models; Greenhouse gases; Earth systems modeling

1. Introduction

Many human activities cause the release of substances that alter the radiative properties of the atmosphere. Projections intended to represent plausible transient climate change due to anthropogenic forcing must, therefore, rely on emissions projections produced by models of economic activity and technological change. Such projections of changes in economic and technological forces are, however, subject to considerable uncertainty. The evaluation of uncertainty in economic and technological factors and the effects on forecasts of carbon dioxide emissions has a relatively long history

(e.g., Nordhaus and Yohe, 1983; Reilly et al., 1987) but the emissions forecasts associated with particular uncertainty limits, heretofore, have not been used to force complex climate models.

A major advance over the past decade has been the development of coupled ocean-atmosphere models combined with development of computational capacity to simulate transient climate change (IPCC, 2001). A second major advance on the atmospheric modeling front has been the coupling of atmospheric chemistry models with climate models so that the complex interactions of greenhouse gases, urban air pollutants, and other substances can be explicitly represented (Wang et al., 1998; Mayer et al., 2000). Economic modeling has made major advances as well, most recently in the ability to consistently model and project the human activities that lead to emissions of the many

*Corresponding author. Tel.: +1-919-843-5010, fax: +1-919-962-5824.

E-mail address: mort@unc.edu (M.D. Webster).

substances that affect climate directly or indirectly (Babiker et al., 2001; Reilly et al., 1999; IPCC SRES).

These advances in economic and climate modeling make it timely, therefore, to reconsider uncertainty in emissions projections. In this paper, we describe the development of a consistent set of emissions scenarios with known probability characteristics based on projections of human activities over the next 100 years.¹ To produce these scenarios we make use of recent developments in uncertainty techniques (Tatang et al., 1997) and apply them to the Emissions Prediction and Policy Analysis (EPPA) model (Babiker et al., 2001), a computable general equilibrium model (CGE) of the world economy that projects the major greenhouse gases as well as other climatically or chemically important substances. We compare our results to the scenarios generated for the Intergovernmental Panel on Climate Change (IPCC) Special Report on Emissions Scenarios (SRES, 2000).

Section 2 begins with a brief discussion of uncertainty analysis and details of our approach. We then present the resulting distributions of emissions. Finally, we develop specific emissions scenarios with known probability characteristics and simulate resulting climate change using the MIT Integrated Global Systems Model (IGSM), comparing them to the SRES results also simulated through the MIT IGSM (Prinn et al., 1999; Reilly et al., 1999).

2. Uncertainty analysis

There are two broadly different ways to approach the problem of forecasting when there is substantial uncertainty: uncertainty analysis (associating probabilities with outcomes) and scenario analysis (developing “plausible” scenarios that span an interesting range of possible outcomes). Both approaches are evident in climate assessments, most notably the recent IPCC reports. Authors for the IPCC Third Assessment Report (TAR) were encouraged to quantify uncertainty as much as possible (Moss and Schneider, 2000). The IPCC Special Report on Emissions Scenarios (SRES, 2000) used the plausible scenario approach, described as a “story line” analysis where all the scenarios developed were considered “equally valid,” the authors strongly resisting an assignment of quantitative or qualitative likelihoods to scenarios.

There can be great benefit to a “story line” approach as it allows one to explore in detail how particular sets of assumptions produce different or similar outcomes. One advantage is that in assessments involving a set of

authors with widely diverging views, it is typically easier to present scenarios without attaching likelihoods. The scenario or “story line” approach allows scenarios from experts with widely varying “world views” to be considered “equally valid”, avoiding deadlock.

The alternative approach, uncertainty analysis, requires identification of the critical uncertain model parameters, quantification of the uncertainty in those parameters in the form of probability distributions, and then sampling from those distributions and performing model simulations repeatedly to construct probability distributions of the outcomes. With this approach, one can quantify the likelihood that an outcome falls within some specified range.

In the end, the difference between formal quantitative uncertainty analysis and the story line scenario approach is not whether a judgment about likelihood of outcomes is needed but rather when and by whom the judgment is made. Scientists can use the tools of uncertainty analysis and their judgment to describe the likelihood of outcomes quantitatively, or the assessment of likelihood can be left to the policy makers and the public who must ultimately decide whether the risks of climate change are great or small. Our views are that (1) it is important for experts to offer their judgment about uncertainty in their projections and (2) formal uncertainty techniques can eliminate some of the well-known cognitive biases that exist when people deal with uncertainty (Tversky and Kahneman, 1974). The evidence is strong that experts and laymen are equally prone to such biases and quantitative approaches can reduce if not eliminate these biases (Morgan and Henrion, 1990).

Finally, the nature of forecasting economic activity and technological development entails that some judgments about the uncertainty in future trends will be subjective, relying on expert elicitation. Our objection to using story-line analysis to describe uncertainty is not that it is subjective, but that it is not the proper method for quantifying uncertainty. Uncertainty analysis should be used when the goal is to quantify uncertainty.

The uncertainty analysis described in this study is able to produce emissions projections that are consistent with underlying economic, demographic, and technological assumptions across substances for any year and over time. It also allows us to recover the underlying parameter values that can lead to a particular case, where they lie in the input distributions we used, and the probability characteristics of the outcome associated with the case. Our approach involves: (1) use of the MIT Emissions Prediction and Policy Analysis (EPPA) model (Babiker et al., 2001, 2000); (2) sensitivity analysis to determine those parameters that are most important for particular outcomes (Webster et al., 2001); (3) development of probability distributions for the parameters chosen for analysis (described in Section 3);

¹ These scenarios are gridded at $1^\circ \times 1^\circ$ latitude–longitude, and are available to interested researchers by contacting the corresponding author.

(4) application of the Deterministic Equivalent Modeling Method (DEMM) approach to produce a polynomial reduced form fit of the EPPA model (Webster et al., 2001; Webster and Sokolov, 2000; Tatang et al., 1997); and (5) Monte Carlo simulation of the reduced form polynomial fit developed using DEMM.

3. Probability distributions of uncertain parameters

The computational demands of the DEMM approach require limiting the number of independently sampled uncertain parameters where possible. Based on sensitivity analysis (Webster et al., 2001), we identified 12 parameters grouped into eight independent sets of probability distributions to sample from, and assume perfect correlation within each set:

- (1) labor productivity growth—all regions correlated,
- (2) AEEI—all regions correlated,
- (3) agricultural sources of CH₄ and N₂O,
- (4) industrial sources of CH₄ and N₂O,
- (5) industrial sources of HFCs, PFCs, and SF₆,
- (6) fossil fuel combustion sources of SO₂, NO_x, CO, NMVOC, BC, OC, and NH₃,
- (7) agricultural sources of SO₂, NO_x, CO, NMVOC, BC, OC, and NH₃, and
- (8) industrial sources of SO₂, NO_x, CO, NMVOC, BC, OC, and NH₃.

We constructed the distributions for uncertain parameters through expert elicitation and from data obtained from the literature. The probability distributions for labor productivity growth and AEEI were obtained by expert elicitation. Five economists² participated in a protocol, each providing fractiles for the distribution for these variables. The five probability distributions for each quantity were then combined by equally weighting each expert's assessment. The distributions of labor productivity were assessed in terms of GDP growth. Separate distributions for labor productivity growth were assessed for each of the EPPA regions, but in this uncertainty study we treat growth in all regions as perfectly correlated. Similarly, distributions for AEEI were elicited from the experts for OECD regions and separately for non-OECD regions, but treated as perfectly correlated during the random sampling (Table 1).

The remaining parameters reflect uncertainties in emissions per unit of economic activity, which we refer to as emissions coefficients. Uncertainties in current emissions of CH₄ (Olivier et al., 1995) and N₂O (Mosier and Kroeze, 1998) from anthropogenic sources are large

²The participating experts were: Henry Jacoby, Richard Eckaus, A. Denny Ellerman, John Reilly, and Mustafa Babiker.

Table 1
Fractiles of initial GDP and AEEI distributions

Region	2.50%	50%	97.50%
Initial GDP growth rate (%/yr)			
USA	1.65	3.34	4.54
JPN	1.22	2.64	3.65
EEC	1.38	2.75	3.72
OOE	1.39	2.79	3.79
EEX	0.70	3.03	5.04
CHN	1.67	5.24	8.51
FSU	1.69	3.32	4.81
IND	1.94	4.84	7.33
EET	1.88	3.84	5.63
DAE	1.34	4.41	7.06
BRA	-0.39	3.20	6.29
ROW	0.37	3.76	6.68
AEEI (%/yr)			
OECD	0.25	0.96	1.54
Non-OECD	0.23	1.13	1.79

Note: GDP rates are for the initial period, after which they approach an asymptotic limit of 1% for OECD regions and 2% for non-OECD regions.

(Table 2) and for N₂O the range of uncertainty differs between agricultural and industrial sources. These ranges are interpreted as one standard deviation from the mean, and beta distributions fit to the uncertainty factors (Table 3).

Alternative scenarios for emissions of HFCs, PFCs, and SF₆ are given in Harnisch et al. (2000). The major uncertainty surrounding these gases is how emissions per unit of economic activity will change in the future as current anthropogenic emissions are relatively well-constrained by measurements of global concentrations. Thus, for these gases, we treated as uncertain the change in their emissions coefficients over time. The time trend was fit to the emissions coefficient data as exponential (HFCs and SF₆) and linear (PFCs) functions. Probability distributions are developed for the parameters of these uncertain time trend functions (Table 3)³.

Current emissions of the other pollutants, including SO₂, NO_x, CO, NMVOCs, and particulates are subject to substantial uncertainty (Table 2). As above, emissions from each source activity are treated as independent, while the emissions of each non-GHG from a given activity is perfectly correlated during sampling (e.g., SO₂ and NO_x from agriculture are correlated). Estimates of the uncertainty in emissions from agricultural and industrial activities (not including fuel combustion) are based on Edgar v2.0 data (Olivier et al., 1995) and Seinfeld and Pandis (1998). We approximate one

³For more details on these and the other parameter distributions, see Webster et al. (2001).

Table 2
Annual global total emission estimates

	Natural	Anthropogenic	Total
CH ₄ [Tg CH ₄]	160 (110–210)	375 (300–450)	535 (410–600)
N ₂ O [Tg N]	9 (4.3–14.7)	7.2 (2.1–19.7)	16.2 (6.4–34.4)
NO _x [Tg N]	19.3 (6–35)	31.1 (16–46)	50.4 (22–81)
SO ₂ [Tg S]	32 (25–40)	70 (69–76)	102 (95–116)
CO [Tg CO]	370 (280–960)	925 (600–1250)	1295 (880–2210)
BC [Tg C]	—	6.5 (1.8–13) ff 7.2 (2–13) biomass	13.7 (3.8–26)
OC [Tg mass]	7.8 (??)	7.5 (0.75–15) ff 44 (4.4–80) biomass	59.3 (5.2–95)

Source: Summarized from Olivier et al. (1995), Seinfeld and Pandis (1998), and Mosier and Kroeze (1998).

Table 3
Fractiles of 1995 global emissions distributions and trends

Emissions				
Parameter	2.50%	50%	97.50%	Units
CH ₄ agric	41.7	163.5	341.0	MT CH ₄ from agricultural sources
CH ₄ indus	37.0	145.2	302.7	MT CH ₄ from industrial sources
N ₂ O agric	0.8	8.4	16.1	MT N ₂ O from agricultural sources
N ₂ O indus	0.3	1.1	1.9	MT N ₂ O from industrial sources
SO ₂ from fossil fuels	10.4	115.2	220.1	MT SO ₂ from fossil fuels
SO ₂ agric	0.7	7.6	14.5	MT SO ₂ from agricultural sources
SO ₂ indus	5.5	31.7	58.0	MT SO ₂ from industrial sources
HFCs trend	−9.8%	0%	14.8%	Annual exponential rate of change relative to reference (%)
SF ₆ trend	−6.8%	0%	4.6%	Annual exponential rate of change relative to reference (%)
PFCs trend	−0.148	0	0.35	Annual rate of departure from reference (Mt/yr)

standard deviation limits in emissions from industrial sources as $\pm 50\%$ of the mean. Uncertainty in emissions from agricultural sources is somewhat wider and skewed towards higher emissions with an upper standard deviation of $+80\%$ of the mean and a lower standard deviation of -40% .

The dominant source of these other pollutants is the combustion of fossil fuels. The emissions coefficients over time for each species is fit as a power series function of GNP per capita⁴

$$ef = a (\text{GNP/capita})^c \quad (1)$$

except for SO₂ emissions, which are fit as an exponential function

$$ef = a \exp(-c (\text{GNP/capita})). \quad (2)$$

⁴ Macroeconomic models such as EPPA do not have detailed descriptions of technologies and their emissions characteristics, but rather represent average characteristics by industrial sector and country. Thus the treatment of uncertainty is at this aggregate level, and the functional approximations of emissions in terms of GDP/capita capture the aggregate characteristics reasonably well.

The values of the parameters a and c are estimated based on cross-sectional data, along with an estimate of the standard error. The uncertainty in the emissions from fuel combustion is then represented as the average standard error for the parameter a in these functions, which is $\pm 60\%$ of the mean. Uncertainty in the evolution of GNP per capita is driven by the uncertainty in labor productivity growth. Together these two uncertainties encompass a wide range of possible future aerosol and pollutant emissions as a function of the growth of the economy and how emissions are reduced as wealth increases (Table 3).

4. Emissions uncertainty results

Using DEMM, we propagate the uncertainty in 8 independent sets of input parameters by estimating reduced form models of EPPA, and performing Monte Carlo simulation on the reduced form model using 10,000 random samples from the parameter distributions. The resulting samples of emissions of each species

at each time period are then used to construct probability distributions.

The resulting uncertainty in greenhouse gas emissions is summarized by the median, \pm one standard deviation (67%), and \pm two standard deviations (95%) for the emissions of each gas, which are compared with emissions from the six representative scenarios from the IPCC SRES (Fig. 1). Although the SRES scenarios do not have an associated probability, it is useful to compare them to our probabilistic bounds. CO₂ emissions from the SRES scenarios spread over much of our 95% range (Fig. 1a). This is not surprising, since socioeconomic models of many types have been used to project CO₂ emissions for nearly two decades, and modeling studies tend to be fairly consistent (Weyant and Hill, 1999). But while the range itself is similar, the distributions are not. The SRES has a lower bias among its scenarios, with four of the six SRES scenarios well below our median emissions in 2100.

Emissions projections of other greenhouse gases are less consistent between our ranges and the IPCCs. One significant difference is that the IPCC assumes that global emissions of all gases are known for 1990–2000, while there is, in fact, considerable uncertainty in current global emissions, particularly emissions resulting from agricultural activities and emissions from developing countries. We find a larger range of uncertainty in non-CO₂ greenhouse gas emissions than the IPCC does. Four of the six N₂O scenarios are near the lower 67% bound while the other two are near the upper 67% bound, and none are close to our mean.

For the F-gases—hydrofluorocarbons, perfluorocarbons, and sulfur hexafluoride—the IPCC has developed four representative scenarios (Fenhann, 2000; SRES, 2000). Their projections of HFC emissions span considerably less than our 67% probability range. The higher HFC emission trajectories in EPPA permit strong increases of emission levels as a consequence of increases of GDP. In contrast, the SRES emissions remain capped because of a prescribed de-coupling of HFCs from increases of GDP due to market saturation. The low HFC emission levels, which are also possible within EPPA, are also not seen in SRES, as its authors seem fairly pessimistic about the potential for emission control through containment and substitution by alternative fluids. For PFCs the authors of SRES seem skeptical about the availability of technological options to reduce PFC emissions from aluminum production eventually leading to PFC-free production. The results are similar for SF₆.

In Fig. 2, we show the uncertainty in emissions of SO₂, NO_x, CO, and non-methane hydrocarbons. As with the greenhouse gases, our probability bounds account for uncertainty in current global emissions of these species as well as economic growth, while the IPCC assumes that current emissions are known. SO₂ emis-

sions, a precursor to sulfate aerosols, are especially important in climate projections because of the strong negative radiative forcing effect of those aerosols. The difference between the SRES projections of SO₂ emissions and our projections is striking. In all six of the representative scenarios, the IPCC projects that after about 2040, SO₂ emissions will begin to steadily decline. The IPCC assumes that policies will be implemented to reduce sulfur emissions, even in developing countries, in all imaginable cases. By contrast, our study imagines that the ability or willingness to implement sulfur emissions reduction policies is one of the key uncertainties in these projections. Accordingly, our 95% probability range includes the possibility of continuing increases in SO₂ emissions over the next century, as well as declining emissions consistent with SRES. Similarly, though not as striking, SRES projections of NO_x, CO, and NMVOC emissions all fall within the lower half of our probability distributions of emissions.

Finally, we project emissions of other climatically relevant substances not treated in the IPCC SRES: black carbon aerosols, organic carbon aerosols, and ammonia. Recently there has been an increased interest in the radiative forcing properties of light-absorbing black carbon or elemental carbon aerosols, primarily produced from incomplete combustion (Hansen et al., 2000). Aerosols in both polluted and remote areas contain a wide range of organic compounds, resulting from direct emissions or secondary chemical production in the atmosphere, that have negative radiative forcing like sulfate. Finally, ammonia emissions are important because the primary form of sulfate and nitrate aerosols are as ammonium salts. While the influence of changing emissions of ammonia and carbonaceous aerosols has not been explicitly formulated in the current version of the MIT climate-chemistry model, we project these emissions for the new version of the IGSM currently being developed (Fig. 3).⁵

5. Scenarios for climate simulations

Quantifying uncertainty in emissions with probability distributions, as illustrated above, is an important step towards treating uncertainty in climate projections and, ideally, the uncertainty in emissions scenarios would be jointly considered with uncertainty in climate models. For many climate models it is not computationally feasible to run hundreds of scenarios, and instead modelers must simulate a selected set of scenarios, such as those developed in the IPCC SRES. Our approach allows us to select scenarios where we can describe the associated likelihoods.

⁵The IPCC does not project emissions of these substances, so there are no comparisons in the figure.

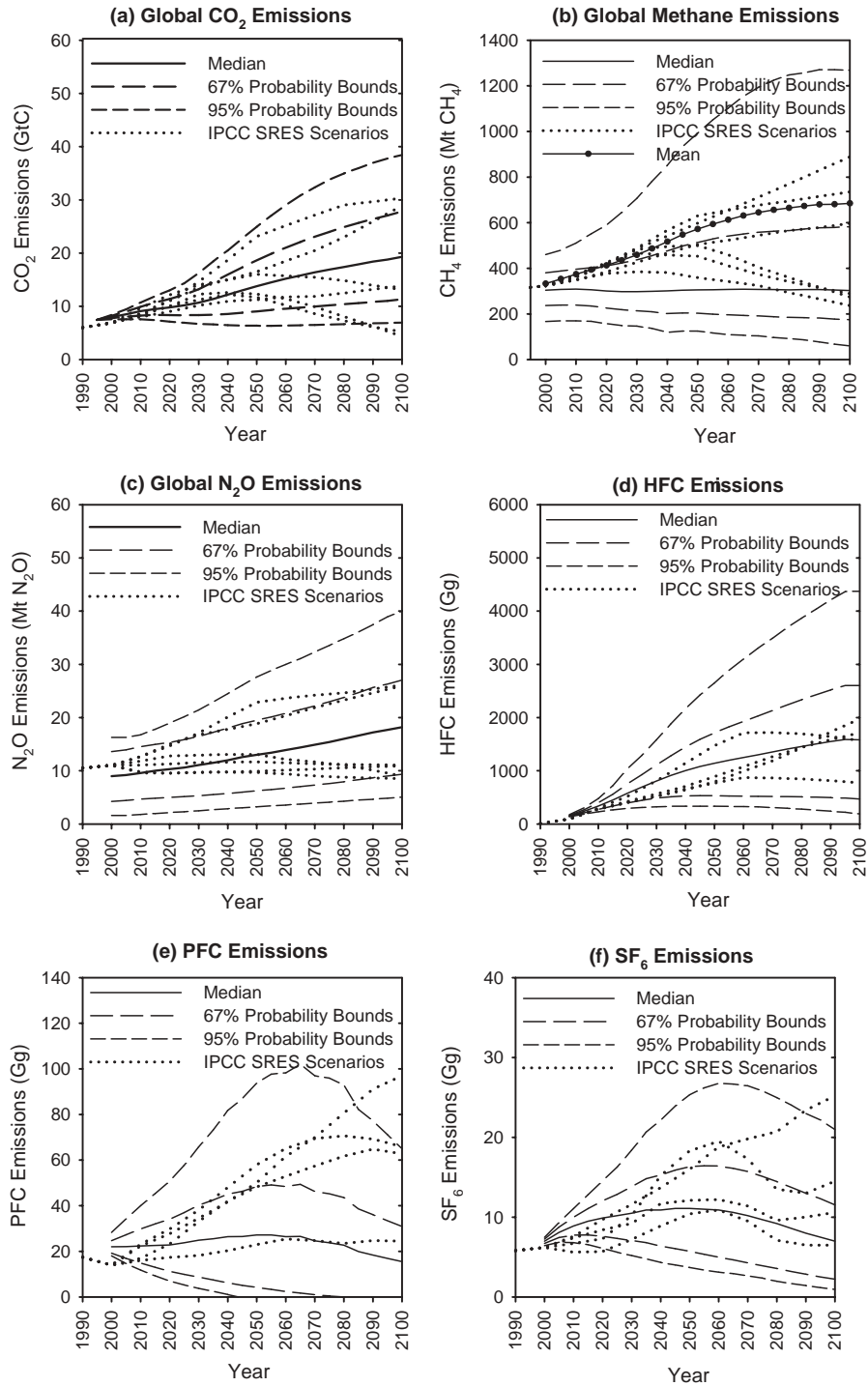


Fig. 1. Emissions of primary anthropogenic greenhouse gases. Panels (a) carbon dioxide, (b) methane, (c) nitrous oxide, (d) HFCs, (e) PFCs, and (f) SF₆. The solid lines show the mean emissions based on 10,000 runs, long dashed lines show ±67%, short dashed lines show ±95% probability bounds, and dotted lines show the emissions from the six representative SRES scenarios.

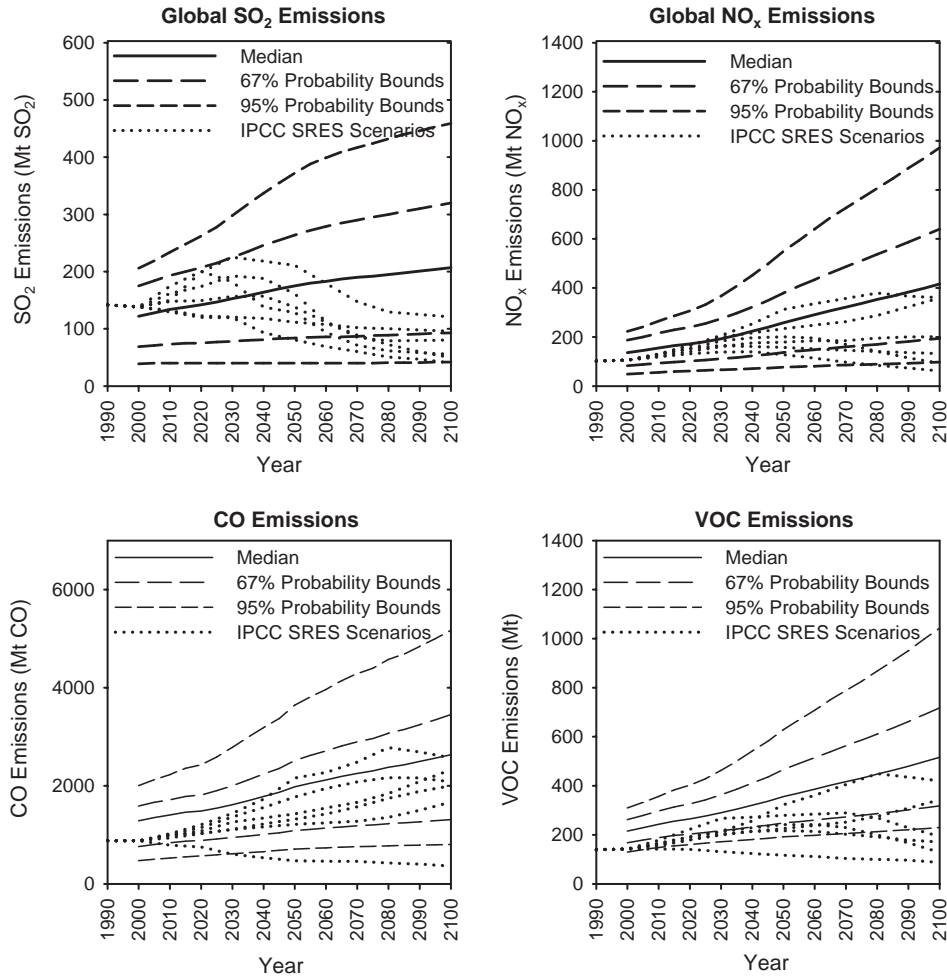


Fig. 2. Emissions of air pollutants. Panels (a) SO₂, (b) NO_x, (c) CO, (d) non-methane hydrocarbons. The solid lines show the mean emissions based on 10,000 runs, long dashed lines show $\pm 67\%$, short dashed lines show $\pm 95\%$ probability bounds, and dotted lines show the emissions from the six representative SRES scenarios.

In designing probabilistically meaningful emissions scenarios for climate models, the multiple climatically or chemically important substances and the correlations among them must be accounted for. If three different probabilities are used for each of the four groups of independently varying emissions in this study, mean, upper 95%, and lower 95%, then there are 3^4 or 81 scenarios that describe every possible combination, an impractically large number of simulations for coupled AOGCMs. Further, this method will result in some scenarios that have extremely low probabilities. For example, choosing the upper 95% value on all four groups has a likelihood of being exceeded of $(0.025)^4 = 3.9 \times 10^{-7}$ or an approximately 1 out of 2,560,000 chance.

We “pare” the decision tree to a few of the most interesting scenarios. The single largest driver of climate

outcomes is CO₂ emissions, so we begin by choosing three emissions scenarios for CO₂ that result in the median, upper 95% and lower 95% emissions levels. In order to keep the overall probability of the scenarios at 2.5% and 97.5%, we fix the other greenhouse gas and non-GHG emissions at their median levels where the median is conditional on CO₂ at median, the upper 95% and the lower 95% emissions. With positive correlation between CO₂ and CH₄ emissions, for example, median emissions of CH₄ conditional on CO₂ at its upper 95% level will be higher than median emissions of CH₄ conditional on CO₂ at its median. This process is illustrated in Fig. 4. Similarly, it is possible to construct other scenarios, such as ones focused on uncertainty in other GHGs or other pollutants conditioned on median outcomes for CO₂ or all GHGs (dashed lines in Fig. 4).

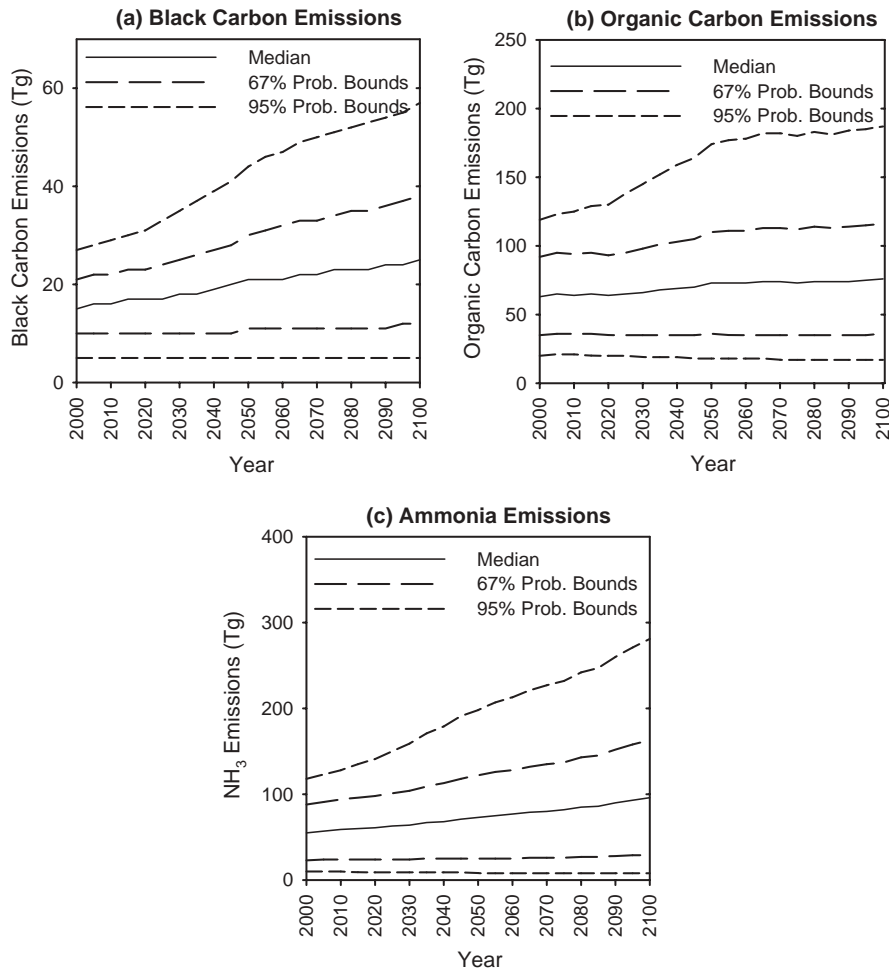


Fig. 3. Emissions of other aerosols and aerosol precursors. Panel (a) black carbon (soot) particulates, (b) organic carbon particulates, and (c) ammonia. The solid lines show the mean emissions based on 10,000 runs, long dashed lines show $\pm 67\%$, short dashed lines show $\pm 95\%$ probability bounds.

6. Climate impacts of representative scenarios

We use the MIT 2D climate-chemistry model to compute the climate impacts resulting from the three representative scenarios presented above. We compare these scenario results to the climate impacts of the six representative SRES scenarios, also as simulated by the MIT climate model. We do not consider, here, the further uncertainties in climate that stem from uncertainties in climate models themselves (Webster and Sokolov, 2000).

The MIT Integrated Global System Model is a set of coupled sub-models that includes the EPPA model as well as submodels that comprehensively simulate atmosphere, ocean, and terrestrial earth systems. Emissions scenarios from EPPA are used as inputs into a coupled chemistry/climate model along with scenarios of natural emissions of GHGs from a Natural Emissions Model

(for wetland CH_4 and natural N_2O emissions) and other natural emissions preprocessor (Prinn et al., 1999; Wang et al., 1998). The chemistry and climate model is a two-dimensional (2D) land-ocean (LO) resolving climate model, which is coupled to a 2D model of atmospheric chemistry and a 2D model of ocean circulations (Sokolov and Stone, 1998; Wang et al., 1998; Wang and Prinn, 1999). In addition, the IGSM includes a 3D urban air chemistry model for treating emissions in urban areas (Mayer et al., 2000). The TEM model of the Marine Biological Laboratory (Melillo et al., 1993; Tian et al., 1999; Xiao et al., 1997, 1998) simulates carbon and nitrogen dynamics of terrestrial ecosystems. These features allow the IGSM to project concentrations of the relevant trace gases, accounting for photochemical processes and the feedback of climate on natural emission sources; radiative forcing from these trace gases; temperature and precipitation at different

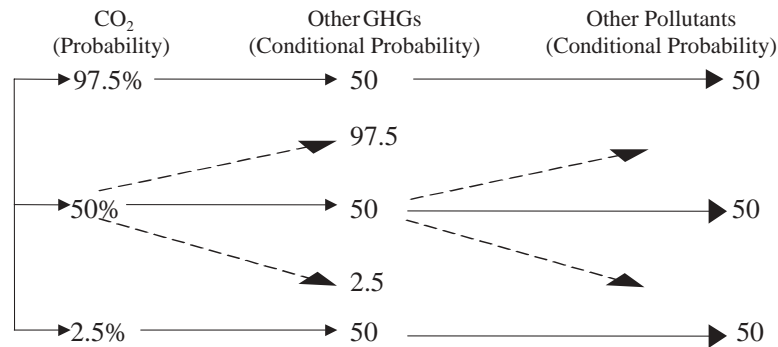


Fig. 4. Probabilities for jointly varying emissions.

latitudes (longitudinally averaged) and global mean; and sea level rise due to thermal expansion of the oceans.

We find that the CO_2 concentration by 2100 reaches 465, 662, and 1090 ppm in the low, median, and high scenarios, respectively (Fig. 5(a)). The SRES span a similar range, from 518 to 965 ppm because of the comparable ranges in CO_2 emissions. Radiative forcing due to CO_2 alone in our scenarios ranges from 3.0 to 8.4 W/m^2 by 2100, and the SRES scenarios result in a similar range. In contrast, the ranges of radiative forcing resulting from other radiatively active substances exhibit greater differences between our scenarios and the SRES. For methane forcing, our scenarios range from 0.4 to 2.3 W/m^2 by 2100, while the SRES covers a smaller range and is biased towards lower forcings, from 0.4 to only 1.5 W/m^2 . Recall that although parameters that drive both CO_2 and CH_4 are at extreme values in the high and low cases, other uncertainties specific to CH_4 are at median values; our range is not as large as a full 95% confidence interval for CH_4 forcing would be. Radiative forcing from N_2O in the SRES covers a more similar range to that of our scenarios, but the SRES are biased towards higher forcings in this case. The combined radiative forcing effects of HFCs, PFCs, SF_6 , and CFCs (not shown) are also biased higher in the SRES: our three scenarios have radiative forcings of 0.2, 0.5, and 0.9 W/m^2 , while the SRES scenarios range from 0.4 to 0.9 W/m^2 .

Perhaps the most important differences are the sulfate aerosol contributions to radiative forcing in our analysis compared with the SRES scenarios. The sulfate forcing in our scenarios is -0.4 , -1.0 , and -1.6 W/m^2 by 2100 in the low, median, and high scenarios, respectively. By contrast, the range of forcings from the SRES scenarios is -0.3 to -0.7 W/m^2 . Our wider range stems from two factors: (1) we represent uncertainty in existing sulfate loading, recognizing that SO_2 emissions come from many sources that are not all monitored and measured with great accuracy; (2) we relate reductions in emissions of SO_2 per unit of fuel combustion and other sources to

growth in per capita income to reflect the growing demand for environmental clean-up with rising incomes that has been observed. As a result of (1), once the wide uncertainty range for emissions in 2000 is represented in the climate chemistry IGSM there is an immediate response, representing uncertainty in current levels of radiative forcing. As a result of (2) and other assumptions about the trend in emissions coefficients, we find the possibility of either increasing or decreasing sulfate aerosol forcing. The SRES scenarios include no uncertainty in current emissions of SO_2 and all scenarios show radiative forcing in 2100 to be below current levels of forcing.

Fig. 5(f) shows the resulting global mean temperature change from 1990 as a result of our three scenarios and the six representative SRES scenarios. Because CO_2 is the largest single driver, the ranges of temperature changes are not extremely different: our scenarios range from 0.9°C to 4.0°C , and the SRES range from 1.3°C to 3.6°C . However, the temperature change in five of the six SRES scenarios is greater than or equal to the temperature change in our median scenario of 2.2°C . The main reason for the difference in the median or central tendency of the two sets of scenarios is the difference in sulfate aerosol forcing. It is important to be clear that the range of global mean temperature change between our low and high scenarios is not a 95% confidence bound on temperature change from the MIT model. To give this range will require applying the methods described here to a full uncertainty analysis of the climate model.

7. Conclusions

Analysis of possible future climate changes should include quantification of the uncertainty in climate projections. After propagating uncertainty through the IGSM, we find that the SRES CO_2 emissions cover much of our 95% confidence range, but are biased

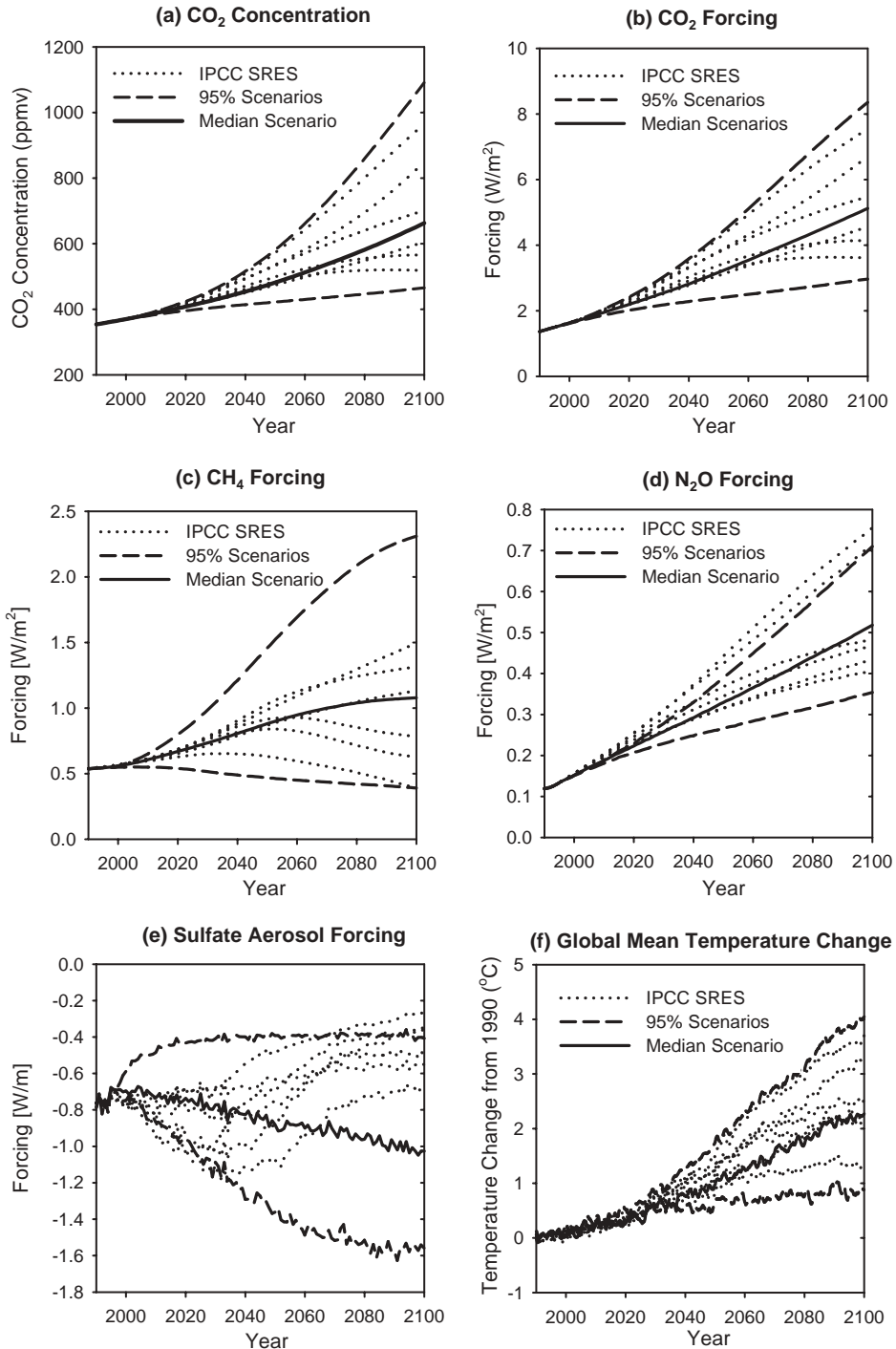


Fig. 5. Concentrations and radiative forcing. Panel (a) CO₂ concentrations, (b) radiative forcing due to CO₂, (c) radiative forcing due to CH₄, (d) radiative forcing due to N₂O, (e) radiative forcing due to sulfate aerosols, (f) global mean temperature change from 1990. Solid lines show median scenario, dashed lines show 95% high and low scenarios as in Fig. 4, and dotted lines show the IPCC SRES scenarios.

towards lower CO₂ emissions by the end of the century compared with our distributions. The differences partly reflect the inclusion of policy effects in some of the SRES scenarios, whereas we have tried to develop probability distributions of emissions under no climate policy. Assessments of the effects of policy would require repeating this exercise under the policy assumption, and then comparing the resulting probability distributions of impacts.

For other greenhouse gases and aerosols, the SRES scenarios tend to encompass much narrower ranges than we find from uncertainty propagation. Further, the SRES emissions are biased higher than our distributions for some species and biased lower for others. One difference is that the IPCC does not include the uncertainty in current emission levels, which is significant in many cases. Finally, the greatest difference between the two methods is found in sulfur emissions. Here, the IPCC has assumed the presence of sulfate reduction policies later in the century seemingly without considering uncertainty in the ability/willingness to implement such policies. In performing the uncertainty analysis, we represent the effect of sulfate reductions as economies increase in wealth, but we have also included the uncertainty in how that relationship will hold for other countries in the future.

As a result of the different methods and assumptions in constructing representative scenarios, we find that the IPCC SRES are biased in the direction of higher global mean temperature change by the end of the next century. This bias towards higher temperatures is partly due to the strongly optimistic assumptions about the reductions in sulfur emissions.

A significant motivation for this study was the perceived desire within the climate modeling community for a small set of scenarios that describe a central tendency (mean or median) and high and low cases that bound an explicit probability. We hope these emissions scenarios provide a useful set of scenarios to study climate uncertainties.

Acknowledgements

Our thanks to our colleagues in the Joint Program for crucial contributions to this paper and to the development of the IGSM model. Particular thanks to Chris Forest, Andrei Sokolov, Richard Eckaus, David Reiner, Henry Jacoby, Denny Ellerman, Asha Rangaraj and an anonymous reviewer. The IGSM has been developed as part of the Joint Program on the Science and Policy of Global Change with the support of a government-industry partnership including a grant from the US Department of Energy's Integrated Assessment Program, Biological and Environmental Research (BER), (DE-FG02-94ER61937) and a group of corporate

sponsors from the United States and other countries. Research on other gases was conducted with funding support from the US Environmental Protection Agency (X-827703-01-0).

References

- Babiker, M., Reilly, J., Jacoby, H., 2000. The Kyoto protocol and developing countries. *Energy Policy* 28, 525–536.
- Babiker, M., Reilly, J., Mayer, M., Eckaus, R., Sue Wing, I., Hyman, R., 2001. The MIT Emissions Prediction and Policy Analysis Model: Revisions, Sensitivities, and Comparisons of Results. MIT Joint Program Report #71, Cambridge, MA. See <http://web.mit.edu/globalchange/www/reports.html#pubs>.
- Fenhann, J., 2000. HFC, PFC and SF₆ emission scenarios: recent development in IPCC special report on emission scenarios. In: van Ham, J., Baede, A.P.M., Meyer, L.A., Ybema, R. (Eds.), *Non-CO₂ Greenhouse Gases: Scientific Understanding, Control and Implementation: Proceedings of the Second International Symposium on Non-CO₂ Greenhouse Gases*. Kluwer Academic Publishers, Dordrecht, Netherlands.
- Harnisch, J., Jacoby, H.D., Prinn, R.G., Wang, C., 2000. Regional emission scenarios for HFCs, PFCs, and SF₆. In: van Ham, J., Baede, A.P.M., Meyer, L.A., Ybema, R. (Eds.), *Non-CO₂ Greenhouse Gases: Scientific Understanding, Control and Implementation: Proceedings of the Second International Symposium on Non-CO₂ Greenhouse Gases*. Kluwer Academic Publishers, Dordrecht, Netherlands, pp. 231–238.
- Hansen, J.E., Sato, M., Ruedy, R., Lacis, A., Oinas, V., 2000. Global warming in the 21st century: an alternative scenario. *Proceedings of the National Academy of Sciences* 97 (18), 9875–9880.
- IPCC, 2001. In: Houghton, J.T., et al. (Eds.), *Climate Change 2001: The Scientific Basis*. Cambridge University Press, Cambridge, 896pp.
- Mayer, M., Wang, C., Webster, M., Prinn, R.G., 2000. Linking local air pollution to global chemistry and climate. *Journal of Geophysical Research* 105 (D18), 22869–22896.
- Melillo, J.M., McGuire, A.D., Kicklighter, D.W., Moore III, B., Vorosmarty, C.J., Schloss, A.L., 1993. Global climate change and terrestrial net primary production. *Nature* 363, 234–240.
- Morgan, M.G., Henrion, M., 1990. *Uncertainty: a Guide to Dealing with Uncertainty in Quantitative Risk and Policy Analysis*. Cambridge University Press, Cambridge, New York.
- Mosier, A., Kroeze, C., 1998. A new approach to estimate emissions of nitrous oxide from agriculture and its implications to the global N₂O budget. *IGACTivities*, no. 12.
- Moss, R.H., Schneider, S.H., 2000. In: Pachauri, R., Taniguchi, T., Tanaka, K. (Eds.), *Guidance Papers on the Cross Cutting Issues of the Third Assessment Report*. World Meteorological Organization, Geneva, pp. 33–57.
- Nordhaus, W.D., Yohe, G., 1983. Future paths of energy and carbon dioxide emissions. In: *Changing Climate*. National Academy Press, Washington DC (Chapter 2.1).

- Olivier, J.G.J., Bouwman, A.F., van der Mass, C.W.M., Berdowski, J.J.M., Veldt, C., Bloos, J.P.J., Visschedijk, A.J.H., Zandveld, P.Y.J., Haverlag, J.L., 1995. Description of EDGAR Version 2.0: A set of global emission inventories of greenhouse gases and ozone depleting substances for all anthropogenic and most natural sources on a per country basis and on $1^\circ \times 1^\circ$ grid. Report no. 771060002. RIVM, Bilthoven.
- Prinn, R., Jacoby, H., et al., 1999. Integrated global system model for climate policy assessment: feedbacks and sensitivity studies. *Climatic Change* 41 (3/4), 469–546.
- Reilly, J., Edmonds, J., Gardner, R., Brenkert, A., 1987. Monte Carlo analysis of the IEA/ORAU energy/carbon emissions model. *The Energy Journal* 8 (3), 1–29.
- Reilly, J., Prinn, R., Harnisch, J., Fitzmaurice, J., Jacoby, H., Kicklighter, D., Melillo, J., Stone, P., Sokolov, A., Wang, C., 1999. Multi-gas assessment of the Kyoto protocol. *Nature* 401, 549–555.
- Seinfeld, J.H., Pandis, S.N., 1998. *Atmospheric Chemistry and Physics*. Wiley, New York.
- Sokolov, A., Stone, P., 1998. A flexible climate model for use in integrated assessments. *Climate Dynamics* 14, 291–303.
- SRES, 2000. In: Nakićenović, N., Swart, R. (Eds.), *Special Report on Emissions Scenarios*. World Meteorological Organization, Geneva.
- Tatang, M.A., Pan, W., et al., 1997. An efficient method for parametric uncertainty analysis of numerical geophysical models. *Journal of Geophysical Research* 102 (D18), 21.
- Tian, H., Melillo, J.M., Kicklighter, D.W., McGuire, A.D., Helfrich III, J.V.K., 1999. The sensitivity of terrestrial carbon storage to historical climate variability and atmospheric CO₂ in the United States. *Tellus* 51B, 414–452.
- Tversky, A., Kahneman, D., 1974. Judgment under uncertainty: heuristics and biases. *Science* 185, 1124–1131.
- Wang, C., Prinn, R.G., 1999. Impact of emissions, chemistry and climate on atmospheric carbon monoxide: 100-year predictions from a global chemistry-climate model. *Chemosphere-Global Change Science* 1 (1–3), 73–81.
- Wang, C., Prinn, R.G., Sokolov, A.P., 1998. A global interactive chemistry and climate model: formulation and testing. *Journal of Geophysical Research* 103 (D3), 3399–3417.
- Webster, M.D., Sokolov, A.P., 2000. A methodology for quantifying uncertainty in climate projections. *Climatic Change* 46 (4), 417–446.
- Webster, M.D., Babiker, M.H., Mayer, M., Reilly, J.M., Harnisch, J., Hyman, R., Sarofim, M.C., Wang, C., 2001. *Uncertainty in Emissions Projections for Climate Models*. MIT Joint Program Report #71, Cambridge, MA. See <http://web.mit.edu/globalchange/www/reports.html#pubs>.
- Weyant, J.P., Hill, J., 1999. The costs of the Kyoto protocol: a multi-model evaluation; introduction and overview. *The Energy Journal (Special Issue)* vii–xliv.
- Xiao, X., Kicklighter, D.W., Melillo, J.M., McGuire, A.D., Stone, P.H., Sokolov, A.P., 1997. Linking a global terrestrial biogeochemical model and a 2-dimensional climate model: implications for the carbon budget. *Tellus* 49B, 18–37.
- Xiao, X., Melillo, J.M., Kicklighter, D.W., McGuire, A.D., Prinn, R.G., Wang, C., Stone, P.H., Sokolov, A.P., 1998. Transient climate change and net ecosystem production of the terrestrial biosphere. *Global Biogeochemical Cycles* 12 (2), 345–360.